Dilute Solution Properties of *cis*-Polyisoprene in Cyclohexane and 1,4-Dioxane

Yoshisuke Tsunashima,* Masukazu Hirata, Norio Nemoto, and Michio Kurata

Institute for Chemical Research, Kyoto University, Uji, Kyoto-fu 611, Japan.
Received July 27, 1987; Revised Manuscript Received October 6, 1987

ABSTRACT: Static light scattering and viscosity measurements were made on five *cis*-polyisoprene fractions of weight-average molecular weight M_w ranging from 0.33×10^6 to 7.2×10^6 in cyclohexane (good solvent) at 25 °C and 1,4-dioxane (Θ solvent) at 34.7 °C. The maximum values for static (=radius of gyration, R_G) and dynamic (=Stokes radius, R_H) expansion factors α_S^3 and α_H^3 of the highest molecular weight sample were 13 and 8, respectively, and were the largest ones obtained so far for light scattering. With these large values, excluded-volume effects and hydrodynamic interaction on chain segments of highly swollen flexible polymers in dilute solutions were tested through the two-parameter theory. The results are the following: (1) The factors α_S^2 and α_H^2 were proportional to $M_w^{1/5}$ for $\alpha_S^2 > 2$–3 and $\alpha_H^2 > 1.5$–2, respectively. Both slopes gave the binary cluster integral (="excluded volume") for a pair of segments β to be 59×10^{-24} cm^3, consistently with each other. (2) The ratios, R_G/R_H and α_S/α_H, were constants, 1.50 and 1.15, respectively, over the entire regions, $4.5 < \alpha_S^3 < 13$ and $3 < \alpha_H^3 < 8.3$, examined. (3) The interpenetration function Ψ versus α_S^3 plot showed a slightly convex-downward curve but was considered to give a constant, $\Psi = 0.19 \pm 0.01$, to within experimental error in $4.5 < \alpha_S^3 < 13$. (4) The viscosity expansion factor α_η^3 gave a relation $\alpha_\eta^3 = \alpha_S^{2.17}$ in all α_S regions measured, and the Flory viscosity factor Φ decreased monotonically as α_S^3 increased with 2.39×10^{23} at $\alpha_S^3 = 1$ and 1.2×10^{23} mol^{-1} at $\alpha_S^3 \sim 13$. (5) As a whole, there is no satisfactory theoretical explanation for experimental findings obtained by present studies except for the α_S versus z relation, where the two-parameter theory seems to hold quantitatively.

Introduction

The asymptotic behavior of linear polymers in dilute solutions in the very large region of the familiar excluded-volume parameter z is the long-lived but unsettled problem in polymer physical chemistry. Only a few attempts have been made through static light-scattering and intrinsic viscosity measurements at α_S^3 larger than 7. Here the quantity α_S denotes the linear expansion factor for root-mean-square radius of gyration of polymers R_G. The representative of these attempts is the studies of Einaga et al.[1-3] They have investigated the behavior of poly(D-β-hydroxybutyrates) (PHB) in trifluoroethanol with the weight-average molecular weight M_w up to 9.1×10^6 [1] and of polystyrenes (PS) in benzene and cyclohexane at $M_w \leq 57 \times 10^6$ [2,3] and tested the two-parameter theory. The results were that (1) α_S^5 becomes proportional to z, as required by the two-parameter theory; however, (2) the interpenetration function Ψ decreases asymptotically to a constant, 0.22, as α_S^3 increases; and (3) the Flory viscosity factor Φ continues to decrease monotonically as α_S^3 increases, and becomes about 1.5×10^{23} mol^{-1} at $\alpha_S^3 = 13$ [1] or 1.7×10^{23} mol^{-1} at $\alpha_S^3 = 11$,[3] implying the breakdown of the two-parameter theory for second virial coefficient A_2 and for intrinsic viscosity $[\eta]$.

Recently we have studied dynamic light scattering properties of *cis*-polyisoprenes (PIP) in dilute solutions of good (cyclohexane)[4] and Θ (1,4-dioxane)[5] solvents and have found that PIP showed dynamically more desirable model-like behavior than PS did. This behavior was especially distinct in good solvents, and it was considered to be due to the high chain flexibility of PIP. There, our PIP fractions ranged in M_w from 0.33×10^6 to 7.2×10^6, and the values of α_S^3 ranged from 4.5 to 13. This upper range of α_S is one of the highest so far examined for linear polymers and is the same as that of PHB.

In the present paper, we therefore describe in detail the results of static light-scattering and viscosity experiments made in this α_S region for PIP in cyclohexane and 1,4-dioxane. With these results and together with our earlier results made for PIP by dynamic light scattering,[4-5] the two-parameter theory for R_G, A_2, $[\eta]$, and the hydrodynamic radius R_H was tested.

Experimental Section

Polymer Samples. Five fractional samples, coded as L-14, L-12, L-15, L-11, and L-16, were made available by Dr. K. Kajiwara. The preparation and fractionation were made as described earlier.[4] The homogeneity was guaranteed by the value of M_w/M_n less than 1.1.[4] The microstructure was determined by applying a 400-MHz ^{1}H NMR spectrometer (Japan Electron Optics Labs., JNM-GX 400) to the solutions of 3 w/v % PIP in $CDCl_3$ at 35 °C. The cis-1,4 content was about 70% for lower molecular weight samples of L-14, L-12, and L-15 but was slightly higher for L-11 and L-16, as shown earlier.[4]

Solvents and Preparation of Solutions. Cyclohexane and 1,4-dioxane (spectrograde, Nakarai Chemicals, Kyoto) were used as a good and a Θ solvent, respectively, for the present study. They were used without further purification since their purity were guaranteed by measuring the refractive indices for D-line in a Pulfrich refractometer at 25.0 °C. Then their refractive index, density, and viscosity were evaluated from the literature values[6] as follows: $n = 1.4220$ (633 nm), $d = 0.77394$ g cm^{-3}, $\eta_0 = 0.898 \times 10^{-2}$ g cm^{-1} s^{-1} for cyclohexane at 25 °C and $n = 1.4137$ (633 nm), $d = 1.0167$ g cm^{-3}, $\eta_0 = 1.019 \times 10^{-2}$ g cm^{-1} s^{-1} for 1,4-dioxane at 34.7 °C.

One solution, called the original solution, was prepared gravimetrically or by filtration for each set of sample/solvent system. Solutions of various concentrations were made by diluting the original solution with the given solvent. Great care was taken to prevent PIP from oxidative degradation in dioxane and from shear degradation in dissolving higher molecular weight samples L-11 and L-16. An antioxidant, about 0.05 w/v % of 2,6-di-*tert*-butyl-*p*-cresol, was added in original dioxane solutions and the container was filled with dry N_2 gas. The containers for L-11 and L-16 solutions were kept still in a dark place for 1 or 2 days, at room temperature for cyclohexane solution or at 38 °C for dioxane solutions. The solutions were then gently stirred mechanically for 1 day, and later the containers were gently shaken intermittently to promote complete dissolution. The entire process took about 2 weeks for L-16 solutions. The dioxane solutions were kept above 32 °C to prevent precipitation of PIP.

Static Light Scattering Measurement. Original solutions and the solvents were made optically clean by centrifugation in a Hitachi preparative centrifuge for all the cyclohexane solutions except the L-16 ones, to which along with the dioxane solutions the filtrations (Millipore filters) were applied. To obtain solutions

0024-9297/88/2221-1107$01.50/0

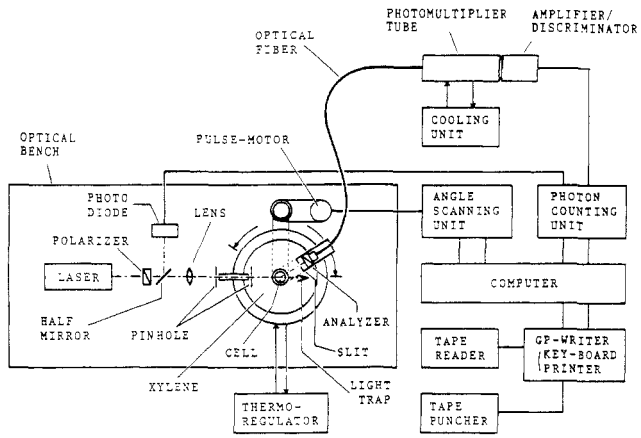

Figure 1. Block diagram of the static light scattering instrument.

of various concentrations, the original solution and the solvent were mixed by weight into the light scattering cells by pipeting (the case of centrifugation) or by direct filtering (the case of filtration). The processes were made in dryboxes under N_2 atmosphere. The cells and pipets were rinsed with spouting condensed methanol in a distillation column. The filter kits were also rinsed beforehand with dust-free fresh water which was obtained through a Barnstead NANOpure-A three-holder system.

The photometer used was the computer-operated photogoniometer, which was designed and constructed in our laboratory.[7] The block diagram is shown in Figure 1. A vertically polarized single-frequency 633-nm line of He–Ne laser (5 mW, Japan Lasers, Model JLH-P50) was focused, through a polarizer, at the center of the measuring cell by an achromatic lens and was attenuated by a light trap placed at zero scattering angle. Part of the incident light was split by a half-mirror and was received on a photodiode, of which the output intensity was digitally counted by the photon counting unit in a computer (System 77-PDP11), and this served as the monitoring intensity. The counting time was synchronized with the sampling time of the scattered intensity emitted from the cell. The measuring cell, a cylindrical Pyrex glass with a brass-bottom pedestal, was immersed in index-matched xylene in the brass bath. The xylene was freed from dust by filtration and its temperature was kept constant to ±0.02 °C by circulated temperature-controlled water (thermostats; MGW-LAUDA, K2RD) in the outer bath surrounding the xylene bath. The scattered light was viewed through a front slit (0.1 mm width × 10 mm high) of the receiving optical system. The slit was covered air tight by a thin glass window and was immersed in the xylene bath. By a pulse motor (Astrosyn Co., Type 23PM-C006), the receiving system was rotated coaxially around the cell over the scattering angle from 0° to 150° at a minimum interval of 0.01°. The scattered light passed through the front slit was then reflected to the vertical direction by a total reflection prism. After passing through another slit (0.4 mm width × 3.0 mm high), an analyzer, and a quartz optical fiber, the light was detected digitally by a photomultiplier (PM) tube (Hamamatsu Photonics, R649)–amplifier/discriminator (Hamamatsu Photonics, C1050) system and was finally counted by the photon counting unit. The PM tube was cooled at −5 °C in order to reduce dark counts and to improve S/N ratios by 1 order of magnitude for those at room temperature. Usually the scattered intensities were accumulated for 10 s per scattering angle. The photon counts obtained were typed out on a GP writer in the form of a Zimm plot.

The calibration of the photometer was pursued by measuring fluorescence emitted from aqueous solution of methylene blue for angles in the range 5–150°. The scattered light due to the 633-nm beam was shut out by a red filter set in front of the optical fiber. The fluorescence intensity multiplied by the sine of the scattering angle was found to be constant to within ±2% in the whole range 5–150°. It assured the precise optical alignments in this photometer. Amounts of stray light at small scattering angles were checked by measuring benzene (spectrograde, Nakarai Chemicals, Kyoto) at 25 °C. They were negligibly small over 20–150° but increased at lower angles; the intensity was 23% and 8% larger at 10° and 15°, respectively, than it should be. However, these amounts were constant at every measurement for seven cells

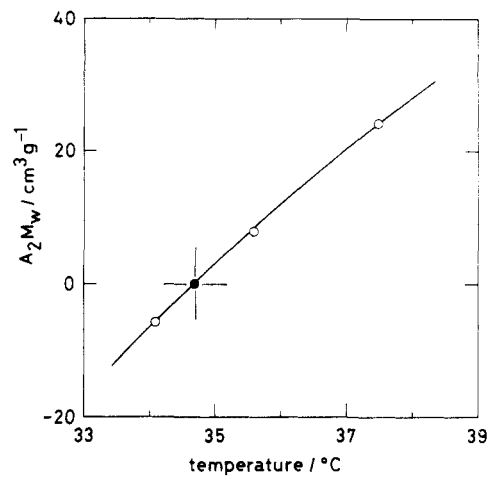

Figure 2. Temperature dependence of A_2M_w for two *cis*-polyisoprene samples L-11 (○) and L-12 (●) in 1,4-dioxane. The thin vertical line indicates the Θ temperature, 34.7 °C.

used in the present work. The photometer was thus found to be reliable at the scattering angles 10–150°. The depolarization ratios ρ_u for benzene, toluene, and carbon disulfide (spectrograde, Merk Co.) at 22 °C were obtained as 0.432, 0.520, and 0.666, respectively, by measuring the ρ_v values. These values agreed to within ±2.5% with the literature values.[8] The absolute calibration of the photometer was made by using benzene, for which the absolute Rayleigh ratio due to Pike et al.,[8] $R_{Uv}(90) = 11.84 \times 10^{-6}$ cm^{-1} (633 nm), was employed.

In the present study, the V_v component was measured for cyclohexane solutions at 25 °C and for 1,4-dioxane solutions at 34.7 °C. The scattering angles were scanned from 10° to 150° at intervals 2° or 5°, the scattering intensity being accumulated for 10 s at each angle. The scanning was repeated several times and averaged at each angle. The refractive index increment of PIP in cyclohexane at 25 °C was taken to be 0.106 cm^3 g^{-1} due to Hadjichristidis and Fetters.[9]

Viscosity Measurements. Measurements were made for five PIP samples in cyclohexane at 25 °C. For higher molecular weight samples, the shear rate effects on the viscosity became significant. Hence we constructed a Cannon–Fenske type of four-bulb spiral capillary viscometer.[10] The viscometer, made of Pyrex glass, consists of a 80-cm^3 liquid reservoir, a spiral capillary of 139 cm length and 0.40 mm inner radius, and four bulbs of different capacity, 0.52, 0.38, 0.27, and 0.18 cm^3, which are aligned vertically from the top to the bottom. The apparent shear rate G can be calculated by the relation $G = ahdg/2\eta_0\eta_r l$ with a and l the inner radius and length of the capillary, respectively, η_r the relative viscosity, g the acceleration of gravity, and h the height of the midpoint between the upper and lower marks for each bulb above the meniscus of the liquid reservoir. The values of h were 8.6, 5.9, 3.4, and 1.2 cm from the top to the bottom bulb and so the values of G in this viscometer ranged from about 15 to 105 s^{-1} for cyclohexane at 25 °C. For lower molecular weight samples, a conventional capillary viscometer of the Ubbelohde type was used, its inner radius of capillary being 0.202 mm. The shear rate was 990 s^{-1} for cyclohexane at 25 °C.

Results

Light Scattering Data in a Θ Solvent. The temperature dependence of the second virial coefficient A_2 was measured for 1,4-dioxane solutions of samples L-11 and L-12 around 34 °C. As shown in Figure 2, the temperature at which A_2 vanishes was 34.7 °C for both samples. Figure 3 shows, as an example, the reciprocal square root of reduced scattering intensity at zero angle $[c/R(\theta)]_{\theta\to 0}^{1/2}$ for L-12 at 34.7 °C as the function of the polymer concentration c. The data points are independent of c and confirm that the PIP is in the ideal state in 1,4-dioxane at 34.7 °C. The temperature, 34.7 °C, is in comparable agreement to 34 ± 1 °C for ca. 70% *cis*-1,4 PIP,[11] ca. 34 °C for ca. 85% *cis*-1,4 PIP,[12] and 35 °C for 70–80% *cis*-1,4 PIP.[13] In

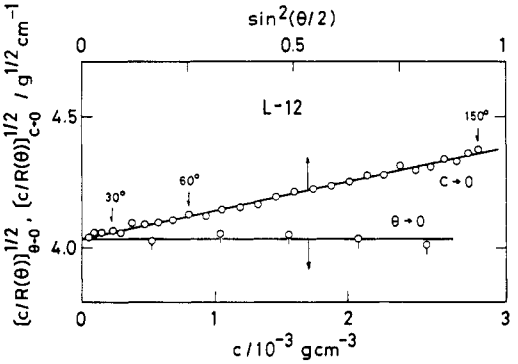

Figure 3. Reciprocal square root of the reduced scattering intensity at zero scattering angle $[c/R(\theta)]_{\theta\to 0}^{1/2}$ as a function of concentration and reciprocal square root of the reduced scattering intensity at zero concentration $[c/R(\theta)]_{c\to 0}^{1/2}$ as a function of $\sin^2(\theta/2)$ for a *cis*-polyisoprene sample L-12 in 1,4-dioxane at 34.7 °C.

Table I
Results of Static Light Scattering Measurements on *cis*-Polyisoprene in Cyclohexane at 25 °C and 1,4-Dioxane at 34.7 °C

	in cyclohexane at 25 °C			in 1,4-dioxane at 34.7 °C	
sample code	M_W, 10^6	R_G, 10^{-6} cm	A_2, 10^{-4} mol cm³ g⁻²	R_{G_0}, 10^{-6} cm	α_S^3
L-14	0.326	3.16	8.04	(1.91)[a]	4.52_5
L-12	0.568	4.33	7.03	2.53	5.07_1
L-15	0.578	4.35	6.77	(2.55)	4.96_5
L-11	2.44	10.5_0	4.74	(5.23)	8.09_6
L-16	7.24	21.0_2	4.37	(9.01)	12.70

[a] The values in parentheses were estimated from the empirical relation $R_{G_0} = 3.35 \times 10^{-9} M_W^{0.50}$ cm.

Figure 3, the angular dependence of $[c/R(\theta)]_{c\to 0}^{1/2}$ is also shown for L-12. These data are represented well by a straight line over the entire angular region from 15° to 150°. The slope gave the value $\langle S^2\rangle_{z_0}^{1/2} = R_{G_0} = 2.53 \times 10^{-6}$ cm. The value agreed to within ±1% with Hadjichristidis et al.'s result[11] in the region $3.9 \times 10^5 < M_w < 2.20 \times 10^6$. Their and our present data are represented well by the relation

$$R_{G_0} = 3.35 \times 10^{-9} M_w^{0.50\pm0.02} \quad \text{cm} \qquad (1)$$

In Table I, the values of R_{G_0} are summarized.

Light Scattering Data in a Good Solvent. In Figures 4 and 5 are illustrated the data on cyclohexane solutions of the sample L-11, the second-highest molecular weight PIP investigated in the present study. In the figures hereafter, the polymer concentration was expressed in a relative unit, c_{rel}, to the original solution concentration c_0 and its absolute value was given in each figure caption. The filled circles in Figure 4 show the concentration dependence of the relative reciprocal square root of reduced scattering intensity $[c_{rel}/R(\theta)]^{1/2}$ at zero angle ($\theta \to 0$). The linear extrapolation of these data points to zero concentration, shown by a solid line, gave the weight-average molecular weight $M_w = 2.44 \times 10^6$ and $A_2 = 4.74 \times 10^{-4}$ mol cm³ g⁻². The unfilled circles in Figure 4 show the angular dependence of $[c_{rel}/R(\theta)]^{1/2}$ for five different concentrations and for the zero concentration ($c \to 0$). The linear extrapolation of the latter ($c \to 0$) data for angles between 10° and 50° gave $M_w = 2.44 \times 10^6$ and $R_G = 10.5 \times 10^{-6}$ cm. This R_G value was checked by another method proposed by Fujita.[14] As shown by the unfilled circles in Figure 5, the data points on the Fujita plot follow a straight line (a dotted line) over the wide range of the relative Fujita's valiable $Z_{rel}(u)$. The range extends to the angles

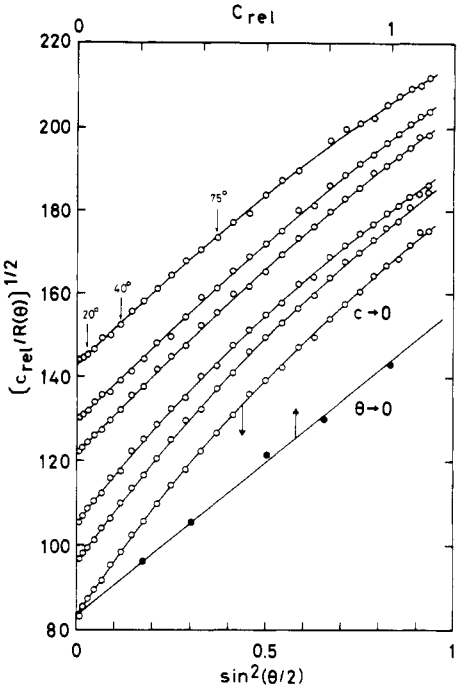

Figure 4. Relative reciprocal square root of the reduced scattering intensity $[c_{rel}/R(\theta)]^{1/2}$ for five different concentrations and its infinite-dilution value $[c_{rel}/R(\theta)]_{c\to 0}^{1/2}$ as a function of $\sin^2(\theta/2)$ and zero-angle value $[c_{rel}/R(\theta)]_{\theta\to 0}^{1/2}$ as a function of relative concentration c_{rel} for second-highest molecular weight *cis*-polyisoprene sample L-11 in cyclohexane at 25 °C. Polymer concentrations are 6.22_6 ($=c_0$), 4.91_4, 3.77_6, 2.28_0, and $1.33_0 \times 10^{-4}$ g cm⁻³ from top to bottom.

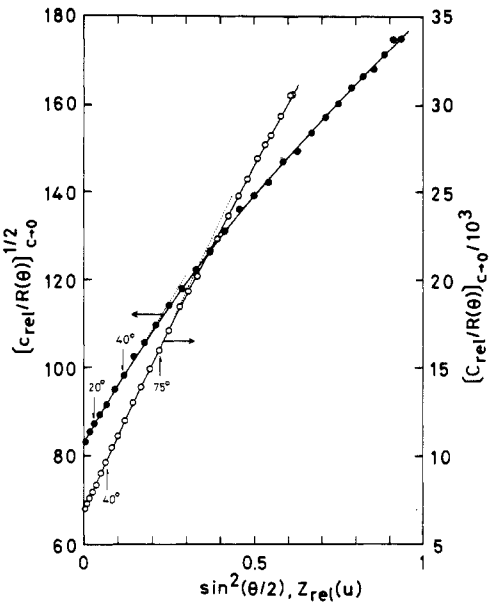

Figure 5. Comparison between square-root plots, $[c_{rel}/R(\theta)]^{1/2}$ versus $\sin^2(\theta/2)$, and Fujita's plots, $c_{rel}/R(\theta)$ ($=y_{rel}^{-1}(u)$) versus $Z_{ref}(u)$, for infinite-dilution values. The data shown in Figure 4 were used. Here $u = \sin^3(\theta/2)$ and $Z(u) = [y(u)u^{4/3}]^{-1}\int_0^u y(u)\,du$: (●) square-root plot; (○) Fujita's plot.

between 10° and 80° and is much wider than that for the usual square-root plot, which is again shown by the filled circles in Figure 5. The R_G value thus estimated by the Fujita plot agreed to within ±1% with the above-mentioned value for the square-root plot.

For other samples, only the extrapolated data at zero angle and at zero polymer concentration are illustrated in Figures 6 and 7, respectively. In Figure 7, the angular dependences of $[c_{rel}/R(\theta)]_{c\to 0}^{1/2}$ are shown for scattering

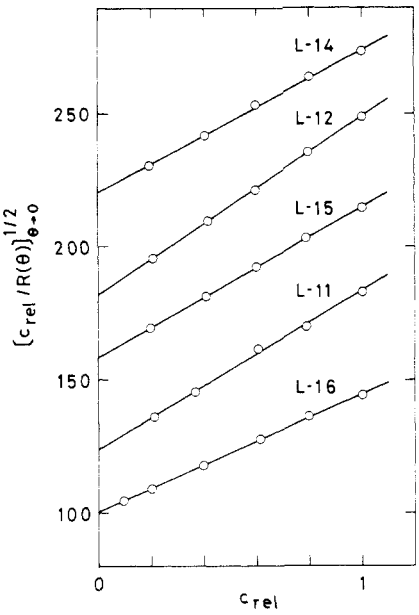

Figure 6. Zero-angle values $[c/R(\theta)]_{\theta\to 0}^{1/2}$ plotted against relative concentration c_{rel} for five *cis*-polyisoprene samples in cyclohexane at 25 °C. The data points are shifted upward by 60 (L-14), 70 (L-12), 30 (L-15), and 40 (L-11). The original polymer concentrations, $c_0 \times 10^4$ g cm^{-3}, are 12.74 (L-14), 15.05 (L-12), 11.21 (L-15), 6.22_6 (L-11), and 1.57_7 (L-16).

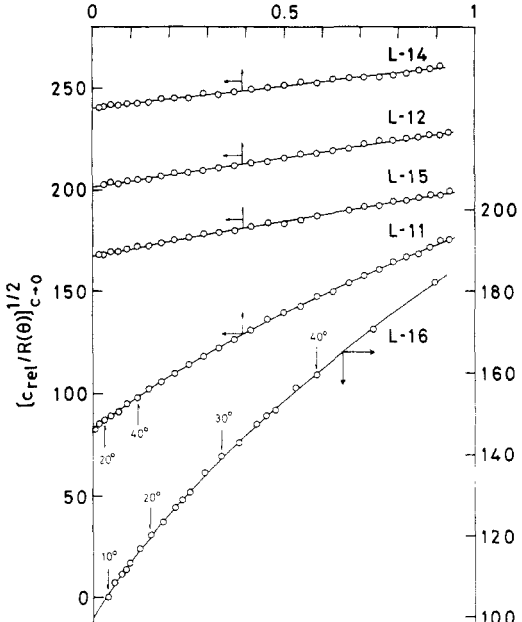

Figure 7. Infinite-dilution values $[c_{rel}/R(\theta)]_{c\to 0}^{1/2}$ plotted against $\sin^2(\theta/2)$ for five *cis*-polyisoprene samples in cyclohexane at 25 °C. The data points are shifted upward by 80 (L-14), 90 (L-12), and 40 (L-15).

angles between 10° and 150° for four samples except L-16, the highest molecular weight PIP in the present study. For L-16, the angular dependence is shown only for angles below 50°. It displays a curvature even around 10–20°. Hence, the values of R_G for L-16 were determined from the Fujita plot where the data points at angles between 10° and 20° were extrapolated linearly to zero angle. The values of M_w, R_G, and A_2 thus determined are summarized in Table I.

In Figure 8a, the value of R_G in cyclohexane at 25 °C and in 1,4-dioxane at Θ temperature are plotted against

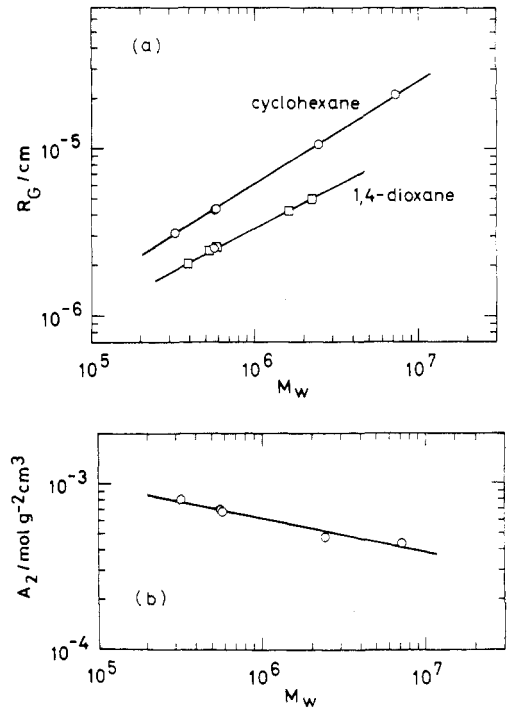

Figure 8. (a) Molecular weight dependence of root-mean-square redius of gyration, R_G, for *cis*-polyisoprene in cyclohexane at 25 °C and in 1,4-dioxane at Θ temperature: (○) in cyclohexane at 25 °C and in 1,4-dioxane at 34.7 °C (present data); (□) in 1,4-dioxane at 34 °C (Hadjichristidis et al.[11]). (b) Molecular weight dependence of the second virial coefficient, A_2, for *cis*-polyisoprene in cyclohexane at 25 °C.

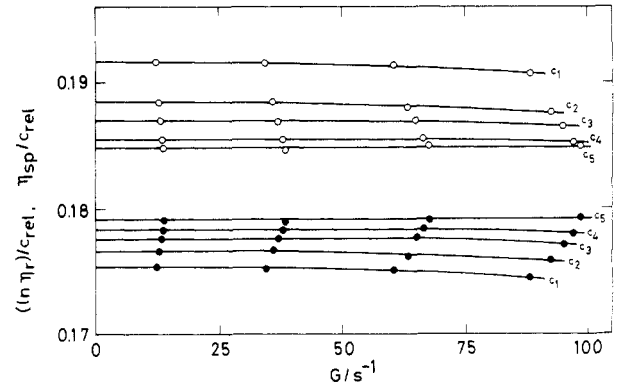

Figure 9. Dependence of η_{SP}/c_{rel} (unfilled circles) and $(ln\eta_r)/c_{rel}$ (filled circles) on apparent shear rate G for highest molecular weight *cis*-polyisoprene sample L-16 in cyclohexane at 25 °C. Polymer concentrations are $c_1 = 0.8330 \times 10^{-4}$, $c_2 = 0.6058 \times 10^{-4}$, $c_3 = 0.4760 \times 10^{-4}$, $c_4 = 0.3702 \times 10^{-4}$, $c_5 = 0.2897 \times 10^{-4}$ g cm^{-3}.

M_w. As far as we know, the present data for cyclohexane solutions are the first presentation on the M_w dependence of R_G in *cis*-PIP/good solvent system. The data are fitted well by an empirical equation

$$R_G = 1.35 \times 10^{-9} M_w^{0.61\pm0.01} \text{ cm} \quad (2)$$

The corresponding empirical equation for 1,4-dioxane solutions is given by eq 1, as described already.

The values of A_2 are plotted against M_w in Figure 8b. They are well represented by the following relation:[4]

$$A_2 = 9.80 \times 10^{-3} M_w^{-0.20\pm0.02} \text{ mol cm}^3 \text{ g}^{-2} \quad (3)$$

Its molecular weight exponent −0.20, though containing a little bit larger uncertainties, agrees with the limiting value expected from theories of flexible linear polymers in dilute good solutions. Experimentally, this value has been obtained only in $M_w > 2 \times 10^7$ for PS in benzene[2] and

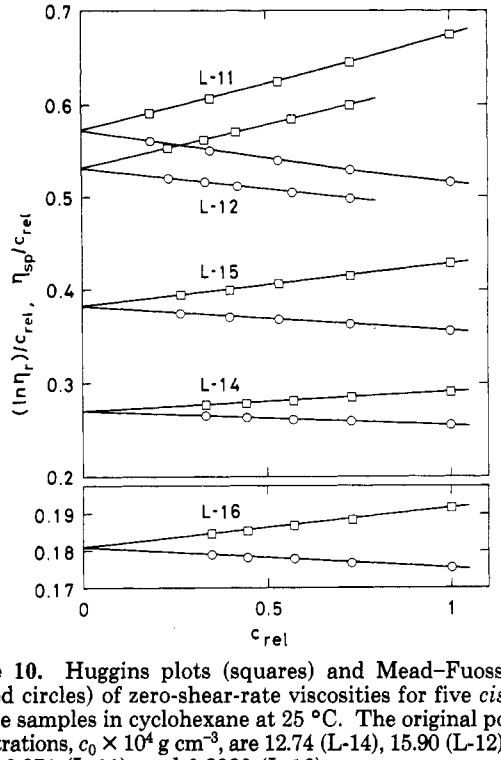

Figure 10. Huggins plots (squares) and Mead–Fuoss plots (unfilled circles) of zero-shear-rate viscosities for five *cis*-polyisoprene samples in cyclohexane at 25 °C. The original polymer concentrations, $c_0 \times 10^4$ g cm^{-3}, are 12.74 (L-14), 15.90 (L-12), 11.21 (L-15), 6.271 (L-11), and 0.8330 (L-16).

Table II
Results of Viscosity Measurements on *cis*-Polyisoprene in Cyclohexane at 25 °C and 1,4-Dioxane at 34.7 °C

	in cyclohexane at 25 °C			in 1,4-dioxane at 34.7 °C		
sample code	$[\eta]$, cm^3 g^{-1}	k'	R_H,[a] 10^{-6} cm	$[\eta]_\theta$,[b] cm^3 g^{-1}	$R_{H\theta}$,[a] 10^{-6} cm	α_H[3]
L-14	212	0.306	2.08_6	75.3	1.43_5	3.07_2
L-12	333	0.338	2.93_3	99.3	1.92_7	3.52_6
L-15	340	0.323	2.94_0	100	(1.95_3)	3.40_3
L-11	918	0.313	6.99_7	206	4.11_7	4.90_9
L-16	2174	0.328	14.00	355	(6.91_5)	8.30_4

[a] Values are taken from our previous works,[4,5] and values in parentheses were estimated by the relation $R_{H\theta} = 2.57 \times 10^{-9} M_W^{0.50}$ cm.[5] [b] Values were estimated by the relation $[\eta]_\theta = 1.318 \times 10^{-1} M_W^{0.50}$.

for PHB in trifluoroethanol.[1]

Viscosity Data in Good Solvent. In Figure 9, the values of $(ln\eta_r)/c_{rel}$ and η_{SP}/c_{rel} at five different concentrations of the highest molecular weight sample L-16 in cyclohexane at 25 °C are plotted against the apparent shear rate G by filled and unfilled circles, respectively. Here η_r means the relative viscosity and η_{SP} the specific viscosity. With the decrease of the concentration, the maximum value of G, below which the data become independent of G, spreads from 40 s^{-1} for $c_1 = 0.8330 \times 10^{-4}$ g cm^{-3} to 100 s^{-1} for $c_5 = 0.2897 \times 10^{-4}$ g cm^{-3}. The value of either $(ln\eta_r)/c_{rel}$ or η_{SP}/c_{rel} at zero shear rate was thus extrapolated with high accuracy. For other samples except L-16, no shear rate dependence of the viscosity was observed.

Figure 10 shows Huggins plots and Mead–Fuoss plots of the zero-shear rate viscosities for five PIP samples in cyclohexane at 25 °C. For each sample, the data are linearly extrapolated to zero concentration with ease and give the common intercept for the two plots. From the intercepts and the Huggins slope, the intrinsic viscosity $[\eta]$ and the Huggins constant k' were determined for the five samples. These results are summarized in Table II. The values of k' are essentially close to $^1/_3$, as was shown for PS of ultrahigh molecular weight.[3]

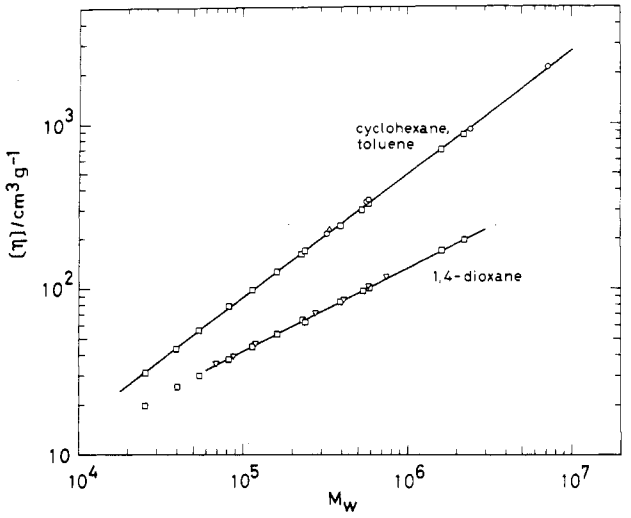

Figure 11. Molecular weight dependence of intrinsic viscosity $[\eta]$ for *cis*-polyisoprene in cyclohexane, in toluene, and in 1,4-dioxane: (○) in cyclohexane at 25 °C (present data); (△) in cyclohexane at 35 °C (Prud'homme et al.[15]); (□) in toluene at 34 °C and in 1,4-dioxane at 34 °C (Hadjichristidis et al.[11]); (▽) in 1,4-dioxane at 31.2 °C (Ansorena et al.[16]). The solid lines represent eq 5 and 6 for good and Θ solvents, respectively.

In Figure 11 are plotted against M_w the values of $[\eta]$ for *cis*-PIP in good solvents, i.e., in cyclohexane at 25 °C (present data) and at 35 °C[15] and in toluene at 34 °C.[11] Our data covering the high M_w region were represented by the relation

$$[\eta] = 1.80 \times 10^{-2} M_w^{0.74\pm0.02} \quad \text{cm}^3\ \text{g}^{-1} \qquad (4)$$

and the plotted points, including ours and others,[11,15] are all fitted closely by the equation

$$[\eta] = 1.59 \times 10^{-2} M_w^{0.747} \quad \text{cm}^3\ \text{g}^{-1} \qquad (5)$$

over the range $2 \times 10^4 < M_w < 10^7$ irrespective of the difference in solvent power or in temperature. The values of $[\eta]$ at Θ temperature, $[\eta]_\theta$, were taken from the reference works made in 1,4-dioxane at 34 °C[11] and at 31.2 °C.[16] As shown in Figure 11, the data points were fitted by the equation

$$[\eta]_\theta = 1.318 \times 10^{-1} M_w^{0.50\pm0.01} \quad \text{cm}^3\ \text{g}^{-1} \qquad (6)$$

if the three data at the lowest M_w region were ignored. The solid lines in the figure are drawn according to eq 5 and 6. By using eq 6, we calculated the values of $[\eta]_\theta$ for our present five samples. The result is listed in Table II.

Discussion

Radius Expansion Factors $\alpha_S(z)$ and $\alpha_H(z)$. According to the two-parameter theory, the static radius expansion factor α_S defined by R_G/R_{G_0} should be a universal function of a single variable z, called the excluded-volume parameter,

$$z = (4\pi R_{G_0}^2/M)^{-3/2}(\beta_S/M_0^2)M^{1/2} \qquad (7)$$

where M_0 is the molecular weight of polymer repeating unit and β_S the binary cluster integral representing the excluded volume of the repeat unit. Evaluation of β_S was proposed by Miyaki et al.[2] They used Domb's asymptotic relation

$$\alpha_S^2 = 1.53 z^{2/5} \qquad (8)$$

which holds at $\alpha_S^2 > 2$–3. In Figure 12, we plotted present data for PIP in the form of α_S^2 versus $M_w^{1/5}$. The data points are actually represented by a straight line passing through the origin. From the slope and together with

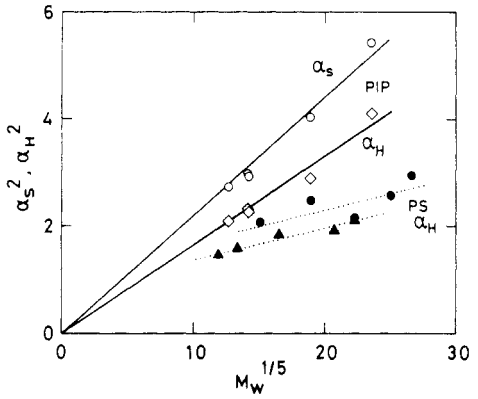

Figure 12. Plots of α_S^2 versus $M_w^{1/5}$ and α_H^2 versus $M_w^{1/5}$ for *cis*-polyisoprene in cyclohexane and plots of α_H^2 versus $M_w^{1/5}$ for polystyrene in benzene and in toluene: (○) and (◇) *cis*-polyisoprene in cyclohexane at 25 °C (present and our previous data[4,5]); (●) polystyrene in benzene at 30 °C with R_{H_θ} in *trans*-decalin at 20.4 °C (our previous data[23,24]); (▲) polystyrene in toluene at 30 °C with R_{H_θ} in cyclohexane at 34.5 °C (Varma et al.[25]). The solid lines fitted to (○) and (◇) represent $\alpha_S^2 = 0.2184\ M_w^{1/5}$ and $\alpha_H^2 = 0.1647 M_w^{1/5}$, respectively. Two dotted lines represent data-fitted empirical ones for polystyrene.

values of $R_{G_0}/M_w^{1/2} = 3.35 \times 10^{-9}$ cm (eq 1) and $M_0 = 68.1$ for PIP, we obtained by using eq 7 the value $\beta_S = 60 \times 10^{-24}$ cm^3. Another method of evaluating β_S is to check the molecular weight independency of β_S in some typical theories on α_S versus z. For this purpose, we chose five of them:

$$\alpha_S^5 - \alpha_S^3 = 2.60z \qquad \text{"original" Flory}^{17} \qquad (9)$$

$$\alpha_S^2 = 0.541 + 0.459(1 + 6.45z)^{0.46} \qquad \text{Yamakawa–Tanaka}^{18} \qquad (10)$$

$$\alpha_S^2 = [1 + 10z + (70\pi/9 + 10/3)z^2 + 8\pi^{3/2}z^3]^{2/15}[0.933 + 0.067 \times \exp(-0.85z - 1.39z^2)] \qquad \text{Domb–Barrett}^{19} \qquad (11)$$

$$\alpha_S^2 = 0.6089 + 0.3911(1 + 6.526z)^{1/2} \qquad \text{Suzuki}^{20} \qquad (12)$$

$$\alpha_S^5 = 1 + 2.85z \qquad \text{Tanaka}^{21} \qquad (13)$$

Substituting experimental values of α_S, R_{G_0}, and M_w into these five equations, and together with eq 7, we computed values of β_S for all five samples of PIP. The eq 11–13 gave better constancy in β_S with the result that $\beta_S = (58 \pm 5) \times 10^{-24}$ cm^3. Thus, the values of β_S obtained by above two methods agree well with each other. The value is about 2 times larger than 30×10^{-24} cm^3 for PS in benzene at 25 °C.[22] This difference seems to be unexplainable from only the difference between the volumes of monomeric unit for PIP and PS in the solvent molecules and suggests some interaction between the monomeric units or/and the monomeric unit and the solvent. This point will be discussed in the forthcoming paper. With $\beta_S = 59 \times 10^{-24}$ cm^3, we calculated z for all five samples of PIP and plotted the values of α_S^2 against z in Figure 13. The plotted points are located well on Suzuki, Domb–Barrett, and Tanaka equations at large z. It is of interest to note that quantitatively the same result has been obtained for PS in benzene.[2] Very recently, Muthukumar and Nickel[46] have proposed the most accurate α_R (the end-to-end distance expansion factor)–z relation of all two-parameter calculations, which covers the full range of $z > 0$ by the formula $\alpha_R^2 = (1 + 7.524z + 11.06z^2)^{0.1772}$. However, no relation was given for α_S^2/α_R^2 there; we could only say that their α_S^2 versus $z^{2/5}$ curve may be located fairly below the Y–T curve in Figure 13. (As shown in the α_R^2 versus $z^{2/5}$ plots in Figure 4 of ref 46, their theoretical values of α_R^2 are much smaller than those of Y–T in all values of $z > 0$.)

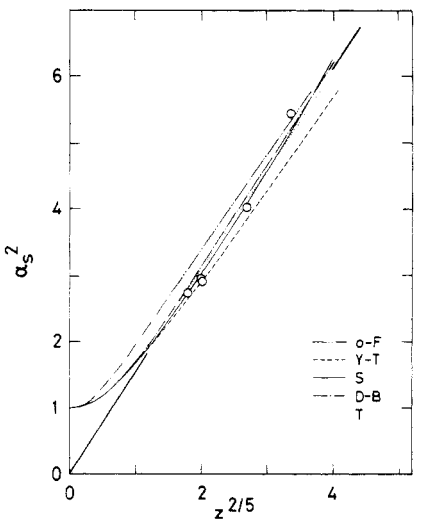

Figure 13. Plots of α_S^2 versus $z^{2/5}$ for *cis*-polyisoprene in cyclohexane at 25 °C. The various lines represent theoretical predictions: (–··–) original Flory equation;[17] (–·–) Domb–Barrett equation;[19] (···) Tanaka equation;[21] (–) Suzuki equation;[20] (– – –) Yamakawa–Tanaka equation.[18] The thick solid line represents eq 8.

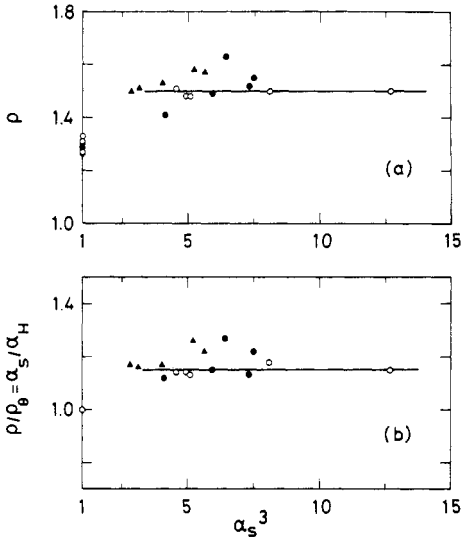

Figure 14. (a) Plots of the dimensionless parameter ρ ($=R_G/R_H$) versus α_S^3 and (b) plots of the ratio ρ/ρ_θ ($=\alpha_S/\alpha_H$) versus α_S^3 for *cis*-polyisoprene and polystyrene in good and Θ solvents: (○) *cis*-polyisoprene in cyclohexane at 25 °C and in 1,4-dioxane at 34.7 °C (present and our previous data[4,5]); (●) polystyrene in benzene at 30 °C and in *trans*-decalin at 20.4 °C (our previous data[23,24]); (▲) polystyrene in toluene at 30 °C and in cyclohexane at 34.5 °C (Varma et al.[25]). The solid lines parallel to the abscissa represent the relations $\rho = 1.50$ and $\rho/\rho_\theta = 1.15$.

In Figure 14, we show the dimensionless parameter ρ and the ratio ρ/ρ_θ ($=\alpha_S/\alpha_H$) as a function of α_S^3 for PIP[4,5] (unfilled circles). Here ρ and ρ_θ are defined by

$$\rho = R_G/R_H \qquad \rho_\theta = R_{G_0}/R_{H_\theta} \qquad (14)$$

with R_H and R_{H_θ} the equivalent hydrodynamic radii of the polymer in good and theta solvents, respectively. R_H is related to the translational diffusion coefficient D_0 as

$$R_H = k_B T/6\pi\eta_0 D_0 \qquad (15)$$

and the hydrodynamic radius expansion factor α_H is defined by $\alpha_H = R_H/R_{H_\theta}$. From Figure 14, it is clear that, for PIP, the values of ρ and ρ/ρ_θ are constants 1.50 and 1.15, respectively, irrespective of molecular weights, as

Table III
Various Characteristic Ratios Defined by Static and Dynamic Properties for *cis*-Polyisoprene in Cyclohexane at 25 °C

sample code	ρ	ρ/ρ_θ (R_G, R_H)[a]	Ψ (A_2, R_G)[a]	α_H/α_η	Φ, 10^{23} mol^{-1} ([η], R_G)[a]	Φ/Φ_0	β_{FSM}, 10^6 ([η], D_0)[a]	$U_{\eta DS}$ ([η], D_0, R_G)[a]
L-14	1.51	1.14	0.202	1.03	1.49	0.622	2.25	0.292
L-12	1.48	1.13	0.208	1.02	1.58	0.661	2.24	0.303
L-15	1.48	1.14	0.205	1.00	1.62	0.685	2.26	0.311
L-11	1.50	1.18	0.182	1.03	1.32	0.551	2.14	0.256
L-16	1.50	1.15	0.184	1.11	1.16	0.482	2.05	0.225

[a] Characteristic values contained in the ratio.

described earlier.[5] In the same figure, the PS data in different solvent systems are also shown by filled symbols, one being obtained in benzene at 30 °C[23] with R_{G_θ} and R_{H_θ} values in *trans*-decalin at 20.4 °C[24] and the other in toluene at 30 °C[25] with Θ values in cyclohexane at 34.5 °C.[25] They show the slight increase with α_S^3 which is caused by the weaker molecular weight dependences of R_H than that of R_G for PS. The difference between PS in benzene and toluene may partly be due to solvent effects on the short-range interaction. Since $\rho/\rho_\theta = 1.15$ for PIP, eq 8 can be converted to the form $\alpha_H^2 = 1.157z^{2/5}$ ($\propto M^{1/5}$) at $\alpha_H^2 > 1.5$–2.3. We plotted the experimental values of α_H^2 against $M^{1/5}$ for PIP in Figure 12. It appears that the asymptotic proportionality between α_H^2 and $M^{1/5}$ is reached at $\alpha_H^2 > 2$, as is expected. The data-fitted solid line which passes through the origin represents the above-mentioned relation $\alpha_H^2 = 1.157z^{2/5}$ with $\beta = 59 \times 10^{-24}$ cm^3. In the similar fashion, the α_H^2 versus $M^{1/5}$ relationship was examined for PS in two solvent systems just mentioned above: benzene[23]/*trans*-decalin[24] and toluene/cyclohexne.[25] As shown in Figure 12 by different filled symbols which distinguish the two solvent systems, the data points follow dotted lines which differ from each other and seem to bend toward $\alpha_S = 1$ at $M_w = 0$. This indicates that the magnitude of M_w for PS samples examined is not high enough to exhibit straight lines which pass through the origin.

Using the value of β(PIP) = 59×10^{-24} cm^3, we evaluated z from eq 7 and plotted α_H^2 for PIP against $z^{2/5}$ in Figure 15 (unfilled circles). The data points are located fairly below theoretical curves T and B and rather follow the solid line passing through the origin, which represents the relation $\alpha_H^2 = 1.157z^{2/5}$ and was obtained from relations $\alpha_S^2 = 1.53z^{2/5}$ and $\alpha_S/\alpha_H = 1.15$. Here, curve T is Tanaka's prediction for the friction expansion factor α_f due to Pade approximation:[21]

$$\alpha_f^5 = 1 + 3.045z \tag{16}$$

where we assumed that $\alpha_H = \alpha_f$. Another curve B represents an approximated closed form obtained from Monte Carlo experiments by Barrett,[26]

$$\alpha_H = (1 + 6.09z + 3.59z^2)^{0.1} \tag{17}$$

With $\beta = 30 \times 10^{-24}$ cm^3 [22] and $R_{G_0}/M_w^{1/2} = 2.80$ (in *trans*-decalin at 20.4 °C[27]) or 2.92 (in cyclohexane at 34.5 °C[25]) $\times 10^{-9}$ cm, PS data were also plotted in Figure 15. The data points (filled symbols) scatter around the solid line and make a further discussion difficult.

It is of interest to note that the experimental value $\rho/\rho_\theta = 1.15$ for PIP in good solvent (Figure 14) lies between (=8% different from) the theoretical values, 1.236 and 1.060, which were obtained[4] by using pseudo-Gaussian and generalized Domb–Gillis–Wilmers segment distributions[45] for swollen chains, respectively. The Monte Carlo value 1.087,[26] obtained with the Domb segment distribution,[45] is also comparable to the PIP value with 6% difference. Tanaka[21] has given $\rho/\rho_\theta = [(1 + 2.85z)/(1 + 3.045z)]^{1/5} \simeq 0.987$ at large z by Pade approximation. Weill and des

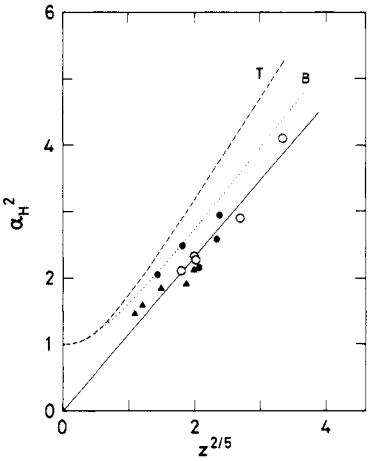

Figure 15. Plots of α_H^2 versus $z^{2/5}$ for *cis*-polyisoprene in cyclohexane and for polystyrene in benzene and toluene. Symbols have the same meaning as in Figure 14. The broken line T and the dotted line B represent the theoretical values from eq 16 by Tanaka[21] and eq 17 by Barrett,[26] respectively. The solid line represent the empirical relation $\alpha_H^2 = 1.157z^{2/5}$.

Cloizeaux[28] have also lead that $\rho/\rho_\theta = \Phi_\theta/\Phi$ from the relation $\alpha_\eta^3 = \alpha_S^2\alpha_H$ with Φ the viscosity constant and α_η the viscosity expansion factor. However, the latter two expectations were less sufficient than the former.

Interpenetration Function $\Psi(z)$. The two-parameter theory predicts that the interpenetration function $\Psi(z)$ defined by

$$\Psi(z) = A_2M^2/(4\pi^{3/2}N_AR_G^3) \tag{18}$$

is a universal function of z, accordingly of α_S. The values of Ψ for PIP in cyclohexane were calculated by using values of A_2 and R_G given in Table I, and are summarized in Table III. They are plotted against α_S^3 in Figure 16 by unfilled circles. The points are fitted approximately by a slightly convex-downward solid curve, where Ψ decreases gradually with increasing α_S^3 and reaches a constant value $\Psi_\infty = 0.18_3$ at $\alpha_S^3 > 8$. However, this slight trend may be within experimental error. From eq 2 and 3, we have $A_2M_w^2R_G^3 = \text{constant} \times M_w^{-0.03\pm0.04}$, and thus it may be better to say that Ψ looks constant, 0.19 ± 0.01, to within the error limits offered, over the whole range of α_S^3 examined. We have three typical calculations which give a constant value of Ψ_∞ at large α_S: 0.1806 by Oono,[29] 0.1969 by Kurata et al.,[30,31] and 0.1658 by Fixman[32] and Casassa and Markovitz.[33] These values are indicated by horizontal bars at α_S^3 over 15. The experimental value 0.19 is close to Kurata's and Oono's values. However, this agreement might be fortuitous, as described below. In Figure 16, we plotted also Ψ values for PS[2,25,27,36] against α_S^3 by filled and cross symbols. It is of interest to note that the PS dta show the convex-downward feature at $\alpha_S^3 < 3$ and seem to reach the asymptotic value $\Psi_\infty = 0.22 \pm 0.01$.[1,3] Recent small-angle neutron scattering data (+) by Huber et al.[36] at extremely small α_S confirm this feature clearly. For Ψ in the smaller α_S^3 region, all the available theories except the

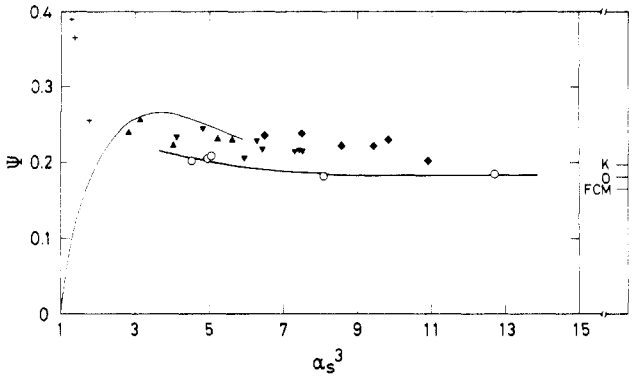

Figure 16. Plots of the interpenetration function Ψ versus α_S^3 for *cis*-polyisoprene in cyclohexane and for polystyrene in benzene and toluene: (○) *cis*-polyisoprene in cyclohexane at 25 °C (present data); (◆) polystyrene in benzene at 25 °C (Miyaki et al.[2]); (▼) polystyrene in benzene at 30 °C (Fukuda et al.[27]); (▲) polystyrene in toluene at 30 °C (Varma et al.[25]); (+) polystyrene in toluene at 20 °C (Huber et al.[36]). All α_S values for PS except (▼) were calculated with data in cyclohexane at 34.5 °C, for (▼) with *trans*-decalin at 20.4 °C. The solid line represents the empirical fit to the data, and the solid thin line represents the results of a computer calculation by Gobush et al.[34] The short horizontal bars shown at $\alpha_S^3 > 15$ indicate the theoretical asymptotic values of Ψ: 0.1969 (Kurata et al.[30,31]); 0.1806 (Oono[29]); 0.1658 (Fixman,[32] Casassa and Markovitz[33]).

one (a thin solid curve in the figure) by Gobush et al.[34] have predicted that Ψ starts from 0 at $\alpha_S = 1$, sharply increases, then soon approaches the asymptotic value. This prediction fails to explain the result for PS. Huber and Stockmayer[35] have very recently explained the decrease of Ψ at small α by the non-Gaussian dependence of chain dimensions on M caused by local chain stiffness and have predicted that $\Psi \propto M^{-1}$ at small M in good solvents. Taking these situations into consideration, Ψ should be described by the theory which gives a global convex-downward feature at $\alpha > 0$. As far as discussions are limited in $\alpha_S^3 > 4$, the values of Ψ for PIP and PS are both constant, though the former is 10–20% smaller than the latter in the magnitude. The difference might be attributed to higher chain flexibility of PIP chains.

Viscosity Expansion Factor α_η. According to the two-parameter theory, the viscosity expansion factor α_η defined by

$$\alpha_\eta^3 = [\eta]/[\eta]_\Theta \tag{19}$$

should be represented by a universal function of α_S and hence z. In Figure 17, we present, on logarithmic scale, the α_η^3 versus α_S^3 relations for PIP in cyclohexane (unfilled circles). The plotted points pass through the origin and have a slope of 0.772, as indicated by the fitted solid line 1. The line gives the relation $\alpha_\eta^3 = \alpha_S^{2.17}$. This is surprisingly close to an uncorrected theoretical relation given by Fujita et al.,[37] $\alpha_\eta^3 = \alpha_S^{2.03}$, but is located far above the corrected one by Shimada and Yamakawa,[38] $\alpha_\eta^3 = \alpha_S^{1.787}$ (S–Y line), which were both proposed for the initial behavior of log α_η^3 versus log α_S^3 at small α_S. Moreover, the empirical line 1 is found to be located fairly below another theoretical curve T, which represents Tanaka's relation

$$3\alpha_\eta^5 = 1 + 2\alpha_S^5 \tag{20}$$

This was obtained by eliminating z from eq 13 for α_S and eq 21 for α_η[21] with Pade approximation

$$\alpha_\eta^5 = 1 + 1.90z \tag{21}$$

On the other hand, the PS data (filled symbols) obtained in benzene[2,3,27] and toluene[25] deviate from the line 1 around log $\alpha_S^3 \cong 0.7$ and shift at log $\alpha_S^3 > 0.8$ to another line 2

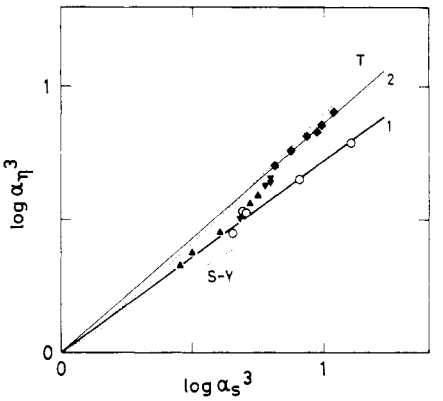

Figure 17. Plots of log α_η^3 versus log α_S^3 for *cis*-polyisoprene in cyclohexane and for polystyrene in benzene and toluene. The data shown by a symbol (◆) represent values by Einaga et al.[3] for polystyrene in benzene at 25 °C. The other symbols are the same as in Figure 16. α_S for PS was calculated the same way as in Figure 16. The dotted lines represent theoretical values: (T) $3\alpha_\eta^5 = 1 + 2\alpha_S^5$ by Tanaka[21]; (S–Y) $\alpha_\eta^3 = \alpha_S^{1.787}$ by Shimada and Yamakawa[38] for small α_S. Two solid lines are the empirical fit to the data; 1, $\alpha_\eta^3 = \alpha_S^{2.17}$ for *cis*-polyisoprene; 2, $\alpha_\eta^3 = \alpha_S^{2.58}$ for polystyrene.

($\alpha_\eta^3 = \alpha_S^{2.58}$) which passes through the origin with the slope 0.861. The data at log $\alpha_S^3 > 0.8$ seem to obey the theoretical line T.

The plotted data for PIP and PS have the same molecular-weight dependences of R_G and $[\eta]$ in the good solvent limit, $R_G \propto M_w^{0.60}$ and $[\eta] \propto M_w^{0.74-0.75}$, as described already in eq 2 and 5 for PIP and in ref 2 and 3 for PS. Hence, the different slopes of log α_η^3 versus log α_S^3 at large α_S^3 in Figure17 indicate that the chain flexibility plays an important role in $[\eta]$ and that the two-parameter theory may break down for $[\eta]$. The breakdown has been revealed recently by Miyaki and Fujita[22] through works for PS in different solvents.

In this connection, it is emphasized that according to the relation

$$[\eta] = 6^{3/2}\Phi R_G^3/M \tag{22}$$

the empirical result for PIP, $R_G \propto M_w^{0.61\pm0.01}$ (eq 2), should give the exponent $\nu = 0.80$ in $[\eta] \propto M_w^\nu$ for the good solvent limit, but eq 5 showed that $\nu = 0.75$. The value 0.8 has seldom been reported in well-documented experimental works for flexible linear polymers with narrow molecular weight distribution such as PS or poly(methyl methacrylate) in good solvents. The present case for PIP confirms again this experimental fact. However, the situation seems to be more serious than in the case of PS since the limiting relation for the translational diffusion, $R_H \propto M_w^{0.6}$, has already been established experimentally for PIP in good solvent,[4] though not for PS (R_H(PS) $\propto M_w^{0.55}$).[23] We can say that $[\eta]$, which associates with rotational motions as well as translational ones, remains unsettled theoretically. The following sections will make clear this situation.

In Figure 18a, we illustrate the behavior of Flory's viscosity parameter Φ/Φ_0 ($=\alpha_\eta^3/\alpha_S^3$) as a function of α_S^3, where Φ_0 is the Φ value at the Θ temperature. Here the data are the same as presented in Figure 17. The data for PIP (unfilled circles) decrease asymptotically with increasing α_S^3 and give $\Phi/\Phi_0 \cong 0.5$ at $\alpha_S^3 \cong 13$, as is empirically fitted by the solid curve 1; $\Phi/\Phi_0 = \alpha_S^{-0.835}$. This relation was obtained from the slope of line 1 for PIP in Figure 17 (plot of log α_η^3 versus log α_S^3). The decrease in Φ/Φ_0 is consistent qualitatively with Einaga et al.'s data for PS[3] (◆) but is not in the magnitude: their PS data approach ca. 0.7 at large α_S^3 along the solid line 2, Φ/Φ_0

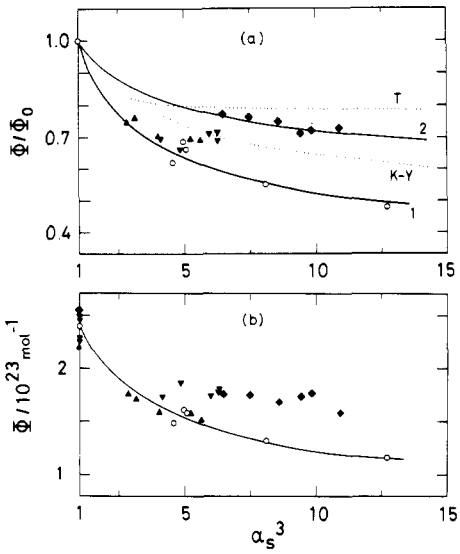

Figure 18. (a) Ratio of Flory viscosity parameters Φ/Φ_0 ($=\alpha_\eta^3/\alpha_S^3$), plotted against α_S^3 for *cis*-polyisoprene in cyclohexane and for polystyrene in benzene and toluene. Symbols are the same as in Figure 17. The solid lines are the empirical fits to these data: 1, $\Phi/\Phi_0 = \alpha_S^{-0.835}$ for *cis*-polyisoprene; 2, $\Phi/\Phi_0 = \alpha_S^{-0.416}$ for polystyrene. The dotted lines represent theoretical values: (T) Tanaka relation;[21] (K–Y) Kurata–Yamakawa relation.[39] (b) Plots of Φ versus α_S^3. Here, the data are the same as in Figure 18a. The solid line is the empirical fit to the data for *cis*-polyisoprene. The data point (◆) at $\alpha_S = 1$ represents Miyaki et al.'s one.[41]

$= \alpha_S^{-0.416}$, which was reduced from line 2 in Figure 17. In Figure 18a, the dotted line T represents Pade approximation for α_η and α_S, i.e., eq 20,[21] and has an asymptotic value of 0.784. Another dotted line K–Y represents Kurata–Yamakawa's semiempirical relation $\Phi/\Phi_0 = \alpha_S^{-0.57}$.[39] Moreover, Oono and Kohmoto[29] and Barrett[26] have given that $(\Phi/\Phi_0)_\infty \cong 0.66$. No theory can explain experimental Φ/Φ_θ for PIP satisfactorily.

Figure 18b shows plots of Φ against α_S^3 for PIP (unfilled circles) and PS (filled symbols). With increase of α_S^3, the data for PIP continue to decrease monotonically from the value $\Phi_0 = 2.39 \times 10^{23}$ at $\alpha_S = 1$ down to around $\Phi \cong 1.2 \times 10^{23}$ at $\alpha_S^3 \cong 13$, as is empirically represented by a solid curve. The Ψ value at large α_S^3 is again far below the PS one, $(1.6–1.7) \times 10^{23}$, at $7 < \alpha_S^3 < 11$. The value of Φ_0 is significantly smaller than the theoretical nondraining values of 2.87×10^{23} mol^{-1} [31] and than Zimm's recent Monte Carlo calculation value 2.51×10^{23},[40] which is attained in a rigid body motion at sufficiently strong internal friction. At present, we have no explanation for this experimental Φ_0 value. Note that the value $\Phi_0 = 2.55 \times 10^{23}$ for PS in cyclohexane at 34.5 °C[41] is in fortuitous agreement with the Zimm value.

Next we examine the behavior of α_η^2 as a function of $z^{2/5}$. In Figure 19, we show this behavior for PIP by unfilled circles. Values of z were estimated by using β(PIP) = 59×10^{-24} cm^3. The data points seem not to pass through the origin as is indicated by the data-fitted solid line, rather showing trends toward $\alpha_S = 1$ at $z = 0$. They are located below the theoretical predictions shown by dotted curves T and B; T is Tanaka's Pade approximation given by eq 21 and B is Barrett's Monte Carlo experiments,[26]

$$\alpha_\eta = (1 + 3.8z + 1.9z^2)^{0.1} \quad (23)$$

In addition, PIP data are far from PS data (filled symbols), which seem to follow roughly on the line T. By the analogy with the α_S^2 or α_H^2 versus $z^{2/5}$ plot, we present in the Figure 19 a thin solid line passing through the origin with the slope 1.05, which was expected from the rough constancy

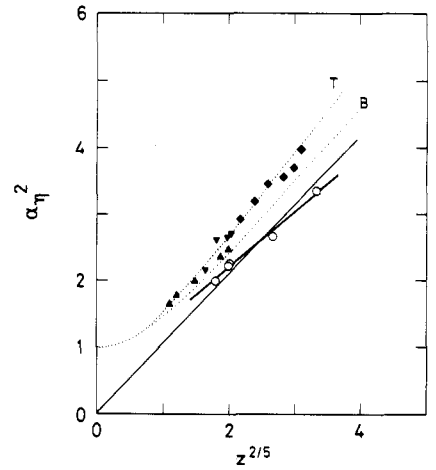

Figure 19. Plots of α_η^2 versus $z^{2/5}$ for *cis*-polyisoprene in cyclohexane and for polystyrene in benzene and toluene. Symbols are the same as in Figure 17. The dotted lines T and B represent Tanaka's relation, eq 21, and Barrett's one, eq 23, respectively.

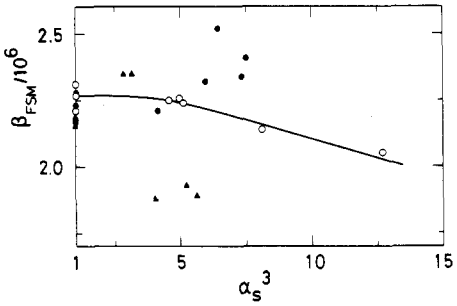

Figure 20. Plots of Flory–Scheraga–Mandalkern factor β_{FSM} versus α_S^3 for *cis*-polyisoprene and for polystyrene in good and Θ solvents. Symbols are the same as in Figure 14. The solid line is the empirical fit to the data for *cis*-polyisoprene.

Table IV
Various Characteristic Ratios Defined by Static and Dynamic Properties for *cis*-Polyisoprene in 1,4-Dioxane at 34.7 °C

sample code	Φ_0, 10^{23} mol^{-1}	$\beta_{FSM,\theta}$, 10^6	$U_{\eta DS,\theta}$
L-14	2.40	2.31	0.413
L-12	2.37	2.27	0.403
L-15	2.38	(2.28)[a]	(0.405)
L-11	2.39	2.21	0.393
L-16	2.39	(2.28)	(0.406)

[a] Values in parentheses were calculated by using values of translational diffusion coefficients at the Θ temperature $D_{0\theta}$ which were interpolated through an empirical relation $D_{0\theta} = 8.68 \times 10^{-5} M_W^{0.50}$ cm^2 s^{-1}.[5]

of α_H/α_η for PIP, 1.04 ± 0.04, irrespective of molecular weight of samples (Table III).

Universal Factors β_{FSM} and $U_{\eta DS}$. Mandelkern, Flory, and Scheraga[42,43] have introduced a factor, β_{FSM}, which is composed of two dynamic properties of $[\eta]$ and friction constant f:

$$\beta_{FSM} = (M[\eta]/100)^{1/3}(\eta_0/f) = (M[\eta]/100)^{1/3}(D_0\eta_0/k_BT) \quad (24)$$

Oono et al.[29,44] have also introduced another factor, $U_{\eta DS}$, which includes $[\eta]$, D_0, and R_G:

$$U_{\eta DS} = [\eta]D_0M\eta_0/k_BTN_AR_G^2 \quad (25)$$

These values of factors were calculated for PIP in good and Θ solvents and are listed in Tables III and IV, respectively. In Figure 20, we plot the values of β_{FSM} for PIP against

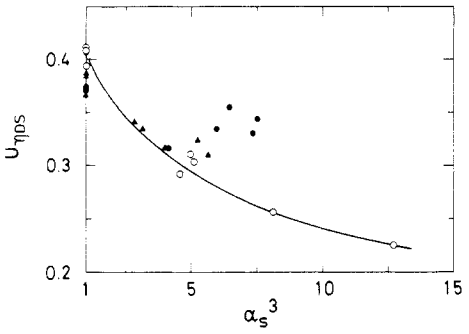

Figure 21. Factor $U_{\eta DS}$ plotted against α_S^3 for *cis*-polyisoprene and for polystyrene in good and Θ solvents. Symbols and the solid line have the same meaning as in Figure 20.

α_S^3 by unfilled circles. It is seen that data points are nearly constant in the small α_S^3 region and then decrease gradually at $\alpha_S^3 > 5$ as α_S^3 increases. This behavior is different from the prediction made through renormalization group techniques by Oono et al.,[29,44] who showed an increase of β_{FSM} from 1.976 at $\alpha_S = 1$ to 2.190 in good solvent limit.

As listed in Table IV, the values of β_{FSM} for PIP at Θ state ($\alpha_S = 1$) were constant irrespective of molecular weight and gave the average value $\beta_{FSM,\Theta} = (2.27 \pm 0.04) \times 10^6$. This value agrees with Zimm's recent one, 2.29×10^6, for rigid-body motions.[40] However, this agreement seems to be accidental because it became clear[4,5] that PIP chains never made complete rigid-body-like motions. For data of PS,[23-25] the β_{FSM} values (filled symbols) at $\alpha_S > 1$ scatter too much to be discussed.

Figure 21 shows α_S^3 dependence of the factor $U_{\eta DS}$ obtained for PIP (unfilled circles). Data points have a value $U_{\eta DS,\Theta} = 0.40 \pm 0.01$ at $\alpha_S = 1$ and then decrease asymptotically down to about 0.22 at $\alpha_S^3 = 13$, as represented by a data-fitted empirical curve. Oono et al.[29,44] have predicted that the value of $U_{\eta DS}$ is 0.321 and 0.270 in Θ state and in good solvent, respectively. However, these values are far from experimental ones. The data for PS[23-25] at $\alpha_S^3 > 1$ again scatter too much to be discussed.

Conclusion

Excluded-volume effects and hydrodynamic interaction on chain segments of highly swollen flexible polymers in dilute solutions were examined through static and dynamic light scattering characteristics and viscosity data obtained on five *cis*-polyisoprene fractions of M_w ranging from 0.33×10^6 to 7.2×10^6 in cyclohexane at 25 °C and 1,4-dioxane at 34.7 °C. The results are the following: (1) The factors α_S^2 and α_H^2 were proportional to $M_w^{1/5}$ for $\alpha_S^2 > 2$–3 and $\alpha_H^2 > 1.5$–2, respectively. Both slopes gave the binary cluster integral (="excluded volume") for a pair of segments β to be 59×10^{-24} cm^3, consistently with each other. (2) The ratios R_G/R_H and α_S/α_H were constants, 1.50 and 1.15, respectively, over the entire regions $4.5 < \alpha_S^3 < 13$ and $3 < \alpha_H^3 < 8.3$ examined. (3) The interpenetration function Ψ versus α_S^3 plot gave a constant value 0.19 ± 0.01 over $4.5 < \alpha_S^3 < 13$. (4) In the entire α_S regions measured, the viscosity expansion factor α_η^3 gave a relation $\alpha_\eta^3 = \alpha_S^{2.17}$, and the Flory viscosity factor Φ decreased asymptotically as α_S^3 increased with 2.39×10^{23} at $\alpha_S^3 = 1$ and 1.2×10^{23} mol^{-1} at $\alpha_S^3 \sim 13$. (5) As a whole, there is no satisfactory theoretical explanation for experimental findings obtained by present studies except for the α_S versus z relation, where the two-parameter theory seems to hold well.

Acknowledgment. We are grateful to Dr. L. J. Fetters for his original preparation and fractionation of the PIP samples and to Dr. K. Kajiwara by whom the samples were available for the present study. We also greatly appreciate Prof. W. H. Stockmayer and Dr. K. Huber for helpful discussion and correspondence.

Registry No. PIP, 9003-31-0; cyclohexane, 110-82-7; 1,4-dioxane, 123-91-1.

References and Notes

(1) Miyaki, Y.; Einaga, Y.; Hirosye, T.; Fujita, H. *Macromolecules* **1977**, *10*, 1356.
(2) Miyaki, Y.; Einaga, Y.; Fujita, H. *Macromolecules* **1978**, *11*, 1180.
(3) Einaga, Y.; Miyaki, Y.; Fujita, H. *J. Polym. Sci., Polym. Phys. Ed.* **1979**, *17*, 2103.
(4) Tsunashima, Y.; Hirata, M.; Nemoto, N.; Kurata, M. *Macromolecules* **1987**, *20*, 1992. The description of the PIP samples must be corrected; they were all prepared by L. J. Fetters and were characterized by his group at Akron University, not by D. Nerger.
(5) Tsunashima, Y.; Hirata, M.; Nemoto, N.; Kajiwara, K.; Kurata, M. *Macromolecules* **1987**, *20*, 2862.
(6) Riddick, J. A.; Bunger, W. B. *Organic Solvents*, 3rd ed.; Wiley Interscience: New York, 1970.
(7) The detailed reports are: Kobayashi, T. Master Thesis, Kyoto University, 1980. Hirata, M. Master Thesis, Kyoto University, 1985.
(8) Pike, E. R.; Pomeroy, W. R. M.; Vaughan, J. M. *J. Chem. Phys.* **1975**, *62*, 3188.
(9) Hadjichristidis, N.; Fetters, L. J. *J. Polym. Sci., Polym. Phys. Ed.* **1982**, *20*, 2163.
(10) Larkins, J. H.; Perrings, J. D.; Shepherd, G. R.; Noland, B. J. *J. Chem. Educ.* **1965**, *42*, 555.
(11) Hadjichristidis, N.; Roovers, J. E. L. *J. Polym. Sci., Polym. Phys. Ed.* **1974**, *12*, 2521.
(12) Poddubnyi, I. Ya.; Ehrenburg, E. G. *J. Polym. Sci.* **1962**, *57*, 545.
(13) Adachi, K., private communication.
(14) Fujita, H. *Polym. J.* **1970**, *1*, 537.
(15) Prud'homme, J.; Roovers, J. E. L.; Bywater, S. *Eur. Polym. J.* **1972**, *8*, 901.
(16) Ansorena, F. J.; Revuelta, L. M.; Guzman, G. M.; Iruin, J. J. *Eur. Polym. J.* **1982**, *18*, 19.
(17) Flory, P. J. *J. Chem. Phys.* **1949**, *17*, 303.
(18) Yamakawa, H.; Tanaka, G. *J. Chem. Phys.* **1967**, *47*, 3991.
(19) Domb, C.; Barrett, A. J. *Polymer* **1976**, *17*, 179.
(20) Suzuki, H. *Macromolecules* **1985**, *18*, 2082.
(21) Tanaka, G. *Macromolecules* **1982**, *15*, 1028; *Ibid.* **1980**, *13*, 1513.
(22) Miyaki, Y.; Fujita, H. *Macromolecules* **1981**, *14*, 742.
(23) Nemoto, N.; Makita, Y.; Tsunashima, Y.; Kurata, M. *Macromolecules* **1984**, *17*, 425.
(24) Tsunashima, Y.; Nemoto, N.; Kurata, M. *Macromolecules* **1983**, *16*, 1184.
(25) Varma, B. K.; Fujita, Y.; Takahashi, M.; Nose, T. *J. Polym. Sci., Polym. Phys. Ed.* **1984**, *22*, 1781.
(26) Barrett, A. J. *Macromolecules* **1984**, *17*, 1561, 1566. Note that the inconsistent values of α_S/α_H were reported; 1.087 in the former and 1.34 ($=P_0/P$, $P = f/6^{1/2}\eta_0 R_G$) in the latter.
(27) Fukuda, M.; Fukutomi, M.; Kato, Y.; Hashimoto, T. *J. Polym. Sci., Polym. Phys. Ed.* **1974**, *12*, 871.
(28) Weill, G.; des Cloizeaux, J. *J. Phys. (Les Ulis, Fr.)* **1979**, *40*, 99.
(29) Oono, Y.; Kohmoto, M. *J. Chem. Phys.* **1983**, *78*, 520. Their values $\Psi = 0.219$ and $\Phi/\Phi_0 = 0.707$ should be read as 0.1806 and 0.661, respectively.
(30) Kurata, M.; Fukatsu, M.; Sotobayashi, H.; Yamakawa, H. *J. Chem. Phys.* **1964**, *41*, 139.
(31) Yamakawa, H. *Modern Theory of Polymer Solutions*; Harper and Row: New York, 1971; Chapters 4, 6, and 7.
(32) Fixman, M. *J. Chem. Phys.* **1962**, *36*, 3123.
(33) Casassa, E. F.; Markovitz, H. *J. Chem. Phys.* **1958**, *29*, 493.
(34) Gobush, W.; Solc, K.; Stockmayer, W. H. *J. Chem. Phys.* **1974**, *60*, 12.
(35) Huber, K.; Stockmayer, W. H. *Macromolecules* **1987**, *20*, 1400.
(36) Huber, K.; Bantle, S.; Lutz, P.; Burchard, W. *Macromolecules* **1985**, *18*, 1461.
(37) Fujita, H.; Tani, N.; Norisuye, T.; Sotobayashi, H. *J. Polym. Sci., Polym. Phys. Ed.* **1977**, *15*, 2255.
(38) Shimada, J.; Yamakawa, H. *J. Polym. Sci., Polym. Phys. Ed.* **1978**, *16*, 1927.
(39) Kurata, M.; Yamakawa, H. *J. Chem. Phys.* **1958**, *29*, 311.
(40) Zimm, B. H. *Macromolecules* **1980**, *13*, 592.
(41) Miyaki, Y.; Einaga, Y.; Fujita, H.; Fukuda, M. *Macromolecules* **1980**, *13*, 588.
(42) Mandelkern, L.; Flory, P. J. *J. Chem. Phys.* **1952**, *20*, 212.

(43) Scheraga, H. A.; Mandelkern, L. *J. Am. Chem. Soc.* **1953**, *75*, 179.
(44) Oono, Y. *Adv. Chem. Phys.* **1985**, *61*, 301. His values of β_{FSM} and U_{nDS} were revised by us, as shown in the text.
(45) For the generalized Domb–Gillis–Wilmers segment distribution $W(r,n) = c_n r^l \exp[-(r/\langle r_n^2\rangle^{1/2})^t]$ and $\langle r_n^2\rangle = An^{2\nu}$, Tsunashima et al.[4] have used that $l = 2.80$, $t = 2.40$, and $2\nu = 1.166$. The pseudo-Gaussian distribution has $l = t = 2$ and $2\nu = 1.2$, and the Domb distribution by Barrett[26] has $l = t$ and $2\nu = 1.2$.
(46) Muthukumar, M.; Nickel, B. G. *J. Chem. Phys.* **1987**, *86*, 460.

Influence of $LiClO_4$ on the Properties of Polyether Networks: Specific Volume and Glass Transition Temperature

Jean-François Le Nest, Alessandro Gandini,* and Hervé Cheradame

Laboratoire de Chimie Macromoléculaire et Papetière, EFP (INPG), BP 65, 38402, Saint Martin d'Hères Cedex, France

Jean-Pierre Cohen-Addad

Laboratoire de Spectrométrie Physique, Université Scientifique, Technologique et Médicale de Grenoble, BP 87, 38402 Saint Martin d'Hères Cedex, France. *Received July 30, 1987*

ABSTRACT: A series of networks based on different polyether chains (PEO homopolymer, block and graft copolymers) joined by different urethane cross-links were prepared. Their specific volume and T_g were determined in the absence and in the presence of $LiClO_4$ as a function of various structural parameters and of salt concentration. Quantitative correlations were obtained and interpreted on the basis of specific interactions between the ether groups and the ionized salt. Chain partitioning and physical cross-linking occurred as a consequence of these associations.

Introduction

The complexation of alkali-metal salts by polyethers has been the subject of many recent publications because of the potential interest of these materials as electrolytes in solid-state batteries.[1,2] However, whereas the interactions between salts and simple ethers, e.g., THF, have been studied in detail, little was known about the behavior of systems involving polymeric media and then only on a qualitative basis.[3] This paper gives an account of a quantitative investigation which complements a previous brief report.[4]

Experimental Section

A wide range of polyether networks was synthesized in the presence or absence of $LiClO_4$. The operations leading to such materials are described below.

Purification and Characterization of Reagents. Commercial polyethers, linear homo- and copolymers, as well as branched copolymers, were purified by reprecipitation in hexane and dried by azeotropic water removal with benzene followed by vacuum treatment at 100 °C for 24 h. This drying technique left only about 100 ppm of moisture, as measured by the Karl Fisher technique. The polyether polyols thus purified and dried were characterized by (i) number-average molar masses (M_n) determined by vapor-pressure osmometry; (ii) polydispersity index, determined by size exclusion chromatography; and (iii) average hydroxyl contents measured by either esterification with acetic anhydride and back-titration of the excess acid or by reaction with *tert*-butyl isocyanate and ^1H NMR counting the relative number of appropriate protons. (iv) Whenever copolymers were used, their composition was termined by ^1H and ^{13}C NMR.

The cross-linking reagents were polyfunctional isocyanates bearing either two such moieties (hexamethylene diisocyanate, HMDI) when used with graft polyether polyols or three NCO groups with linear polyether diols [4,4′,4″-methylidynetris(phenyl isocyanate) and an aliphatic counterpart $OCN(CH_2)_6N(CONH(CH_2)_6NCO)_2$]. The only product that was distilled before use was HMDI. However, the functionality of all isocyanates was checked by the *n*-butylamine method.[5]

The catalyst for urethane formation was commercial dibutyltin dilaurate, employed as received. Finally $LiClO_4$ was vacuum dried at 130 °C for 24 h. Table I summarizes the characteristics of all reagents used.

Synthesis of Networks. The synthesis of salt-containing networks was carried out in purified CH_2Cl_2 following the procedure already described.[6] However, in this study, particular attention was paid to maintain the reagents' concentration constant in all synthesis, namely, 0.43 (total volume of reagents over volume of solution), except for the network based on PEO 200 which was prepared with a volume ratio of 0.65 in order to avoid syneresis problems. These preparations were carried out under stoichiometric conditions (OH/NCO = 1) and the extent of cross-linking was checked by submitting the products to an extraction with CH_2Cl_2. In all instances the soluble fraction did not exceed 1% by weight and was more frequently below 0.5%.

Network Densities. The specific volumes of both saltless and salt-containing networks were determined by pycnometry following two experimental procedures, both involving mercury as nonswelling liquid. One consisted of filling the pycnometer with the network sample and Hg and then vacuum degassing; the other called upon filling the pycnometer containing the sample with mercury under vacuum. All results obtained agreed within less than 1% for each network.

Glass Transition Temperatures. This property was determined by DSC on both saltless and salt-containing networks kept under nitrogen. In order to avoid complications due to the possible crystallization of poly(ethylene oxide) segments in the corresponding networks, all these determinations were conducted according to the following procedure: the samples were placed in a sealed capsule, kept at 100 °C for 1 h, then quenched into liquid nitrogen (to freeze the amorphous conformation), and thereafter analyzed from −165 to 200 °C with a heating rate of 20 °C min^{-1}.

Results and Discussion

Specific Volume. Two sets of experiments were carried out, viz., those on networks without $LiClO_4$ and those on salt–networks systems. All networks were prepared with Desmodur R (see Table I).

Saltless Networks. The variable characterizing the saltless networks in the present context is the cross-link molality m. It was found that the specific volume $\bar{V}$ decreased linearly with the cross-link density, according to the relationship at room temperature:

$$\bar{V} = \bar{V}_0 - 0.11\ m \qquad (I)$$

as shown in Figure 1, where $\bar{V}_0$ is the extrapolated specific

0024-9297/88/2221-1117$01.50/0